Coherent and Incoherent Dihydrogen Dynamics in a Ruthenium Trihydride Complex with the Tris(pyrollyl)phosphine Ligand

Stephan Gründemann[1], Hans-Heinrich Limbach[1*], Venancio Rodriguez[2], Bruno Donnadieu[2], Sylviane Sabo-Etienne[2], and Bruno Chaudret[2*]

[1] Institut für Organische Chemie, Freie Universität Berlin, Takustraße 3, D-14195 Berlin, Germany
[2] Laboratoire de Chimie de Coordination du CNRS, 205, route de Narbonne, 31077 Toulouse Cedex, France

Key Words: Complex Compounds / Hydrogen Transfer / Isotope Effects / Spectroscopy, Nuclear Magnetic Resonance

The ruthenium IV trihydride complex $Cp^*RuH_3(Ppy_3)$ (**1**) accommodating the π-accepting tris(pyrollyl)phosphine ligand has been synthesized by standard methods. This complex exhibits average exchange couplings J of the coherent dihydrogen exchange and average rate constants k of the incoherent dihydrogen exchange which are significantly larger than the corresponding triphenylphosphine and tricyclohexylphosphine analogs. No kinetic HH/HD isotope effects on the incoherent exchange are observed within the margin of error. Using a simple kinetic model involving incoherent vibrational excitation it is shown that in principle both the coherent and the incoherent processes should be related. However, whereas the energy of activation of k corresponds to the barrier of rotation, the energy of activation of the coherent dihydrogen exchange J is much smaller i.e. determined by states well below the barrier. Nevertheless, it is found that chemical modification which reduces the energy of activation of J also reduces the energy of activation of k which demonstrates the relation between both kinds of processes.

1. Introduction

The chemistry of transition metal hydride and dihydrogen complexes has considerably developed during the past few years which resulted in the discovery of novel features of these compounds [1]. The main result is probably the demonstration of the importance of electronic factors for the existence and bonding modes of dihydrogen ligands [1d–f]. Thus, dihydrogen can be stretched, unstretched or electrophilic (even superacidic in specific cases) according to the degree of back-donation from the metal. This has consequences on both the reactivity and the spectroscopic properties of coordinated dihydrogen. The barrier of rotation of coordinated dihydrogen is for example very sensitive to the back-bonding from the metal to dihydrogen [2, 3]. Similarly, some transition metal polyhydrides display very large H-H couplings J in their NMR spectra due to a pairwise coherent quantum mechanical exchange [4]. In addition, they also exhibit incoherent exchange processes characterized by a rate constant k leading to ^{1}H NMR line broadening and coalescence [5]. In several papers it has been postulated that the two phenomena are related to each other [6]; moreover, the J and k appear to be "twins"; if they are of the order of Hz to KHz they influence the ^{1}H NMR spectra, and if they are of the order GHz to THz they appear in the Inelastic Neutron Scattering (INS) spectra [6c]. In addition, the exchange of a pair of deuterons may lead to similar lineshape features in solid state ^{2}H NMR spectra [6d]. Thus, information on the relation between J and k are highly desirable. At present, it is common understanding that the phenomena are indirectly related to the barrier of exchange between the hydrides which in turn depends on the electronic properties of the metal [7].

In order to modify the electron density on transition metal polyhydride or dihydrogen complexes, different approaches were undertaken, namely modification of the ligand sphere [4c, 4f], addition of Lewis acidic coinage cations [4d, 4j] or formation of dihydrogen bonds [7]. For polyhydrides displaying exchange couplings, this increase in electrophilicity of the metal resulted in a strong increase of the magnitude of exchange couplings.

A problem with this appraoch is however that it is very difficult to modify the electronic properties of a complex without modifying the geometry of its coordination environment. The reverse is also true and this has for example been made clear recently by synthesising ruthenium dihydrogen complexes accommodating large bite angle diphosphines [8]. These complexes adopt a cis-geometry for the hydride and dihydrogen ligands and are both electrophilic and unstable. This differs from the similar complexes prepared by Morris which adopt a trans configuration and are stable [9].

However, Molloy recently reported the synthesis of a new series of phosphines containing pyrrollyl substituents ($PPh_{(3-x)}Py_x$, $x = 1$–3) [10]. Within this series, only little modification of the steric properties of the phosphines were observed but a strong electronic modification as deduced from several spectroscopic studies carried out on molybdenum and rhodium complexes [10, 11]. This led us to investigate the electronic influence of this ligand on the spectroscopic properties of polyhydride complexes. For this purpose, we considered the ruthenium trihydride (**1**) depicted in Fig. 1 which contains the Cp*Ru moiety, where $Cp^* = C_5(CH_3)_5$, pentamethylcyclopentadienyl. We note that $Cp^*RuH_3(PR_3)$ with R = cyclohexyl (Cy) (**2**) was the first complex reported to exhibit quantum mechanical exchange couplings [4a]. For **2**, we have recently studied [6c] the coherent and incoherent hydrogen exchange using dynamic NMR spectroscopy. No observa-

*) Authors for correspondence.

  0005-9021/98/0303-0344 $ 17.50+.50/0

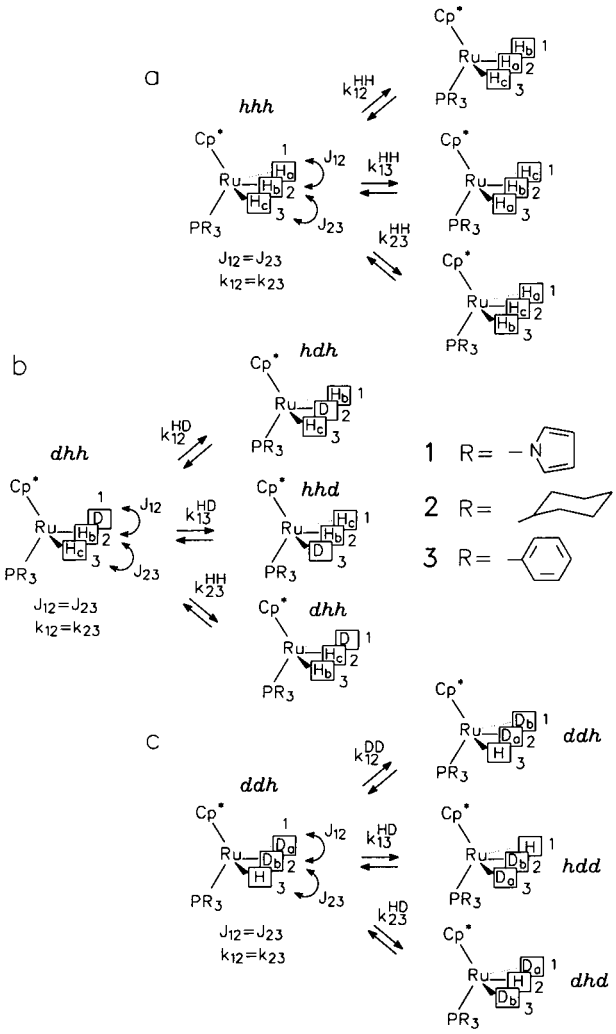

Fig. 1
Chemical formulas and exchange processes in $Cp^*RuH_3R_3$ and its partially deuterated isotopologs. J_{ij} represents the frequency of of the coherent exchange (exchange coupling) of two protons in sites i and j. k_{ij}^{LL}, where L = H, D represents the rate constant of the incoherent exchange of the particles between sites i and j

ble effects of isotopic substitution on the various rate constants of Fig. 1 could be observed. For comparison, we wanted to know how the change of the ligand affects all parameters of the hydrogen exchange processes. This paper is organized as follows. First we describe the synthesis of **1** and of its deuterated analogs, and characterize then the molecule by x-ray analysis and dynamic NMR spectroscopy. Finally, the results are discussed.

2. Experimental

2.1 General

All manipulations were carried out with standard high vacuum or dry argon atmosphere techniques. ^1H, ^{13}C and ^{31}P NMR spectra were recorded on Bruker AC 200, AM 250, AMX 400 or AMX 500 spectrometers. The NMR chemical shifts are reported in ppm, relative to Me_4Si for ^1H and ^{13}C, relative to 85% H_3PO_4 for ^{31}P. $[Cp^*RuCl_2]_2$ [12] and Ppy_3 [10] were prepared according to known methods.

For the low-temperature NMR experiments a liquified CDF_2Cl/CDF_3 mixture (2:1) was used, synthesized as described previously [13]. This solvent is fluid down to 90 K. The sealed NMR samples were prepared on a vacuum line using well-described technique [13]. The NMR spectra were transferred to a personal computer where the lineshape analyses were performed using home-made programs in a similar way as described previously [4j, 6c], based on the quantum-mechanical density matrix formalism of Binsch [14].

2.2 Syntheses

2.2.1 Preparation of $Cp^*RuCl_2P(pyrrolyl)_3$

To a suspension of $[Cp^*RuCl_2]_n$ (600 mg, 1.95 mmol) in 20 ml of ethanol was added tri-N-pyrrolylphosphine (474 mg, 1.95 mmol). After 30 min of reaction the precipitate was filtered, washed twice with 5 ml of ethanol and dried in vacuo. Yield 91%. Anal. Calcd. for $C_{22}H_{27}Cl_2N_3PRu$: C, 49.25; H, 5.08; N, 7.83. Found: C, 48.90; H, 4.84; N, 7.61.

2.2.2 Synthesis of $Cp^*RuH_3P(pyrrolyl)_3$ (**1**)

To a suspension of $Cp^*RuCl_2P(pyrrolyl)_3$ (229 mg, 0.4 mmol) in 10 ml of ethanol at 0 °C was added $NaBH_4$ (107 mg, 3.0 mmol). The cooling bath was removed and the reaction mixture was stirred for 4 h at ambient temperature. After evaporation of solvent the brown residue was extracted with 20 ml of diethyl ether. To the extract 5 ml of ethanol were added and then evaporated just until precipitation starts. After cooling over night, the white crystals of $Cp^*RuH_3P(pyrrolyl)_3$ were isolated by filtration. Yield 82%. Anal. Calcd. for $C_{22}H_{30}N_3PRu$: C, 56.39; H, 6.47; N, 8.97. Found: C, 56.42; H, 6.53; N, 8.94. IR: n(RuH) 1978 cm^{-1}. NMR (C_6D_6) d: (^1H)– 9.29 (d, J_{HP} = 21.7 Hz, RuH), 1.73 (d, J_{HP} = 1.9 Hz, Cp*), 6.22 (m or pseudo-triplet, 6H), 6.75 (m or overlapping doublet of pseudo triplets, 6H). ($^{31}P\{^1H\}$) 129.1 s. ($^{13}C\{^1H\}$) 49.4 (s, $C_5(CH_3)_5$), 108.3 (s, C_5), 117.5 (d, J_{CH} = 6.1 Hz, pyrrolyl), 125,6 (d, J_{CH} = 6.9 Hz, pyrrolyl).

2.2.3 Deuteration of $Cp^*RuH_3P(pyrrolyl)_3$ (**1**)

To a suspension of $Cp^*RuCl_2P(pyrrolyl)_3$ (500 mg, 0.93 mmol) in 15 ml of ethanol at 0 °C was added $NaBD_4$ (273.17 mg, 6.52 mmol). The cooling bath was removed and the reaction mixture was stirred for 4 h at ambient temperature. After evaporation of solvent the brown residue was extracted with 30 ml of diethyl ether. To the extract 5 ml of ethanol were added and then evaporated until a white crystalline precipitate was obtained. It was filtered, washed with ethanol and dried in vacuo. Yield. 80%.

2.3 X-Ray Structure Determinations

The data was collected on a Stoe Imaging Plate Diffraction System (I.P.D.S.) equipped with an Oxford Cryosystems cooler device. The crystal-to-detector distance was 80 mm, crystal decay was monitored by measuring 200 reflections by image. The final until cell parameters were obtained by least-squares refinement of 5000 reflections, any consequent fluctuations of the intensity were observed over the course of the data collection.

The structure was solved by direct methods (SIR92) [15] and refined by least-squares procedures. Hydrogen atoms attached to carbons were located on a difference Fourier maps, but they were introduced in calculation in idealized positions d(C-H) = 0.96 Å, their atomic coordinates were recalculated after each cycle of refinement, they were given isotropic thermal parameters 20% higher than those of the C atoms to which they were attached. The hydrogen atoms H, H′ and H″ attached to Ru were isotropically refined. All non-hydrogens atom were anisotropically refined.

Least-squares refinements were carried out by minimizing the function $\sum w(|F_o| - |F_c|)^2$, where F_0 and F_c are the observed and calculated structure factors. A weighting scheme was used in the last refinement cycles, where weights are calculated following the expression $w = w'\,[1 - \{\Delta\,(F)/6\,\sigma(F_0)\}^2]^2, w' = 1/\left(\sum_{r=1}^{3} A_r T_r(X)\right)$, $X = F_c/F_{cmax}$ [16]. The model reached a good convergence with the functions: $R = \sum(\|F_0| - |F_c\|)/\sum |F_0|, R_w = [\sum w(\|F_0| - |F_c\|)^2/\ \sum w(|F_0|)^2]^{1/2}$, having values listed in Table 2.

Table 1
Crystal data and data collection for the compound: $C_{22}H_{30}N_3PRu$ (**1**)

Crystal data	
Chemical Formula	$C_{22}H_{30}N_3PRu$
Fw	468.55
Crystal system	Monoclinic
Space group	I 2/a
a/(Å)	22.214(2)
b/(Å)	8.4392(8)
c/Å)	23.944(3)
α/(°)	90
β/(°)	100.81(1)
γ/(°)	90
Cell volume (Å^3)	4409
Z; D (g·cm^{-3})	8; 1.41
μ (cm^{-1})	7.79
F_{000}	1925.5
Crystal color	yellow pale
Crystal size (mm)	0.57·0.13·0.07
Crystal form	thin plate
Radiation type	MoK_α
Data collection method	phi rotation
Temperature/(K)	180
Reflections collected	13870
Reflections merged	3272
R_{av}	0.086
θ_{max} (°)	24.2

Table 2
Refinement parameters for the compound: $C_{22}H_{30}N_3PRu$ (**1**)

Refinement	
Refinement on	F_o
R	0.034
R_w	0.041
Abs.corr	none
Weighting scheme	Chebyshev
Coeff.Ar	1.66; 0.155; 1.21
Goodness of fit[a])	1.05
No of reflections used	2911
Observation criterion	[I>1.0σ(I)]
No parameters refined	257

[a]) $\sum w\,(|F_o - F_c|)^2/(N_{obs} - N_{params})]^{1/2}$

Further details of the Data Collection and Refinement Parameters are given in Tables 1 and 2. All calculations were performed with the aid of the soft CRYSTALS [17] running on a personal computer. The drawing of the molecule was realized with CAMERON [18] and the atomic scattering factors for the neutral atoms were taken from International Tables for X-Ray Crystallography [19].

A supporting information concerning the X-Ray structure are available on request from the Director of the Cambridge Crystallographic Data Center, 12, Union Road, GB-Cambridge CB21EZ, on quoting the full journal citation.

3. Results

3.1 Characterization of $C_{22}H_{30}N_3PRu$ (1)

The reaction of $[Cp^*RuCl_2]_2$ [12] with one equivalent of tri-n-pyrrolylphosphine (Ppy_3) produces the ruthenium III complex $Cp^*RuCl_2(Ppy_3)$ similar to other complexes of similar formulation but involving different phosphines [20]. Reduction by $NaBH_4$ in ethanol affords after appropriate treatment the trihydride $Cp^*RuH_3(Ppy_3)$ (**1**) as a white crystalline material. **1** shows two Ru-H stretching frequencies at 2009 and 1978 cm^{-1} in infrared and a hydride signal as a doublet at –9.29 ppm (J_{PH} = 21.7 Hz) at room temperature.

An X-ray crystal structure analysis was carried out at 180 K in order to evaluate the effect of the ligand on the structure of this polyhydride. The results are shown in Fig. 2 and Tables 1 and 2.

3.2 Dynamic ^{1}H NMR Spectroscopy

In order to detect possible quantum mechanical exchange couplings as in the related complexes [20b, 21] we carried out a low-temperature ^{1}H NMR study of **1** and of partially deuterated **1** in freons between 300 K and 130 K. The superposed experimental and calculated signals of the hydride region are shown in Fig. 3. At room temperature we observe a single doublet for all hydrogen nuclei, where

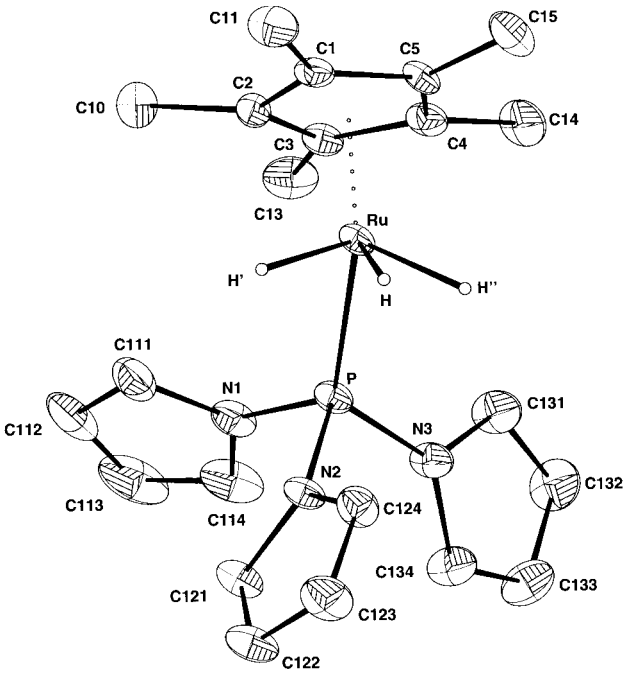

Fig. 2
Molecular structure of $Cp^*RuH_3(Ppy_3)$ (**1**) at 180 K; selected bond lengths (Å) and angles (°): Ru-H: 1.57(4); Ru-H′: 1.60(4); Ru-H″: 1.55(2); Ru-P: 2.1798(8); Ru-Cl: 2.232(3); Ru-C2: 2.273(3); Ru-C3: 2.295(3); Ru-C4: 2.273(3); Ru-C5: 2.235(3); H′-Ru-H: 62(2); H-Ru-H″: 63(2); H′-Ru-H″: 121(3); H-Ru-P: 91(2); H′-Ru-P: 82(2); H″-Ru-P: 78(2)

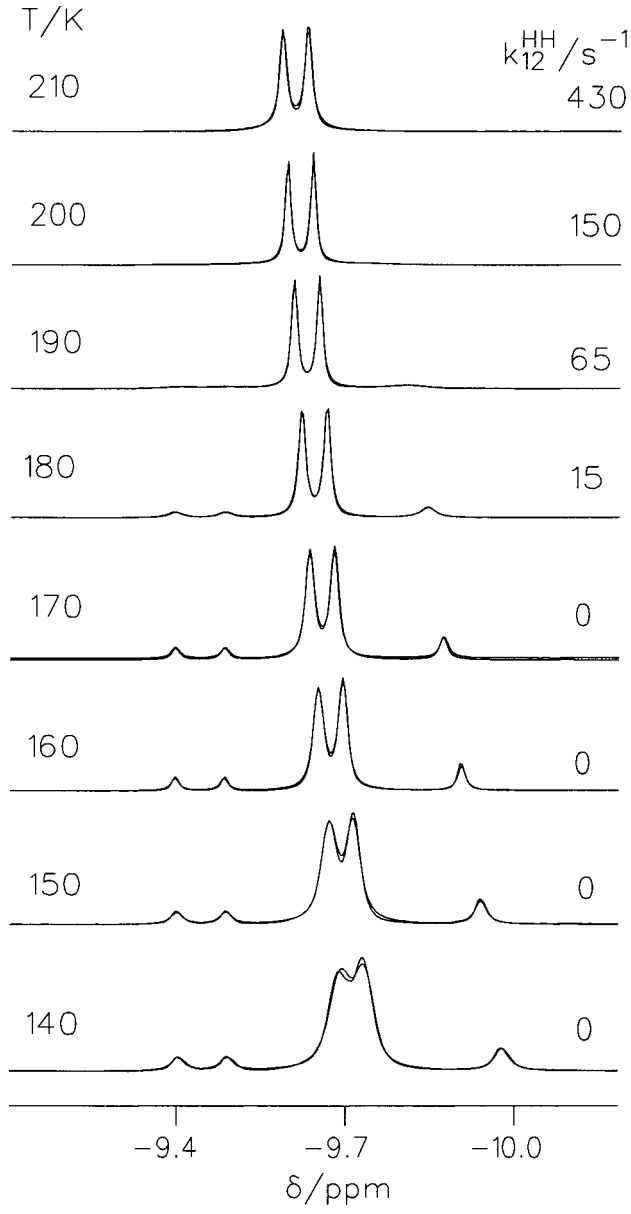

Fig. 3
Superimposed temperature dependent experimental and calculated 500 MHz ^{1}H NMR hydride signals of $Cp^*RuH_3(Ppy_3)$ (**1**) dissolved in $CDClF_2$-CDF_3 (2:1)

the doublet splitting arises from a scalar coupling with the nearby ^{31}P nucleus as confirmed by ^{1}H NMR experiments in the presence of ^{31}P broadband decoupling. As the temperature is decreased, we observe a broadening of the hydride signal near 190 K and the appearance at 180 K of a high-order signal splitting pattern involving a surprising small number of lines which reduce to a trio in the presence of ^{31}P decoupling. The distance between the outer lines increases as the temperature is further decreased. Similar spectra have been observed for $Cp^*RuH_3(PPh_3)$ [21] and are due to the presence of an AB_2X spin system with very large coupling constant between spins A and B, labeled here as J_{12} according to Fig. 1.

In order to detect possible effects of deuteration on the parameters of the exchange we studied additionally a sample deuterated to about 35% in the hydride sites by ^{1}H NMR. As depicted in Fig. 4, the sample exhibits not only signals for **1** but also for **1**-d and **1**-d_2. In the slow exchange two signals are identified for **1**-d_2, a doublet arising from **1**-hdd and a singlet from **1**-dhd, whereas **1**-d contributes an ABX pattern for **1**-hhd and a doublet for **1**-hdh. The actual assignment was assisted by ^{31}P broadband decoupling.

The calculated spectra of Figs. 3 and 4 depend on the following parameters. As the both outer hydride sites are magnetically equivalent the line shape in the ^{1}H NMR spectrum depends on the chemical shifts ν_1 and ν_2 of the two hydrogen sites, the exchange couplings J_{12} between the inner and outer hydrogen nuclei, the scalar coupling constants of the hydrogen nuclei with the nearby ^{31}P nucleus J_{1P} and J_{2P}, and the rate constant k_{12}^{HH} and in the case of **1**-d and **1**-d_2 on k_{12}^{HD} of the incoherent dihydrogen exchange as defined in Fig. 1. The parameters of a possible direct exchange between the hydrogen sites 1 and 3 can not be determined because of their magnetic equivalence.

The results of the lineshape analyses are assembled Table 3. The dependence of the parameters of the coherent and incoherent exchange on temperature can be expressed as

$$\pi J_{12} = 10^{5.7} \exp\left(-5.1\,\mathrm{kJ\,mol^{-1}}/RT\right)\mathrm{Hz},$$
$$140\,\mathrm{K} \le T \le 180\,\mathrm{K} \text{ for } \mathbf{1}\text{−h},$$
$$J_{12} = 3000\,\mathrm{Hz} \text{ at } 180\,\mathrm{K} \qquad (1)$$

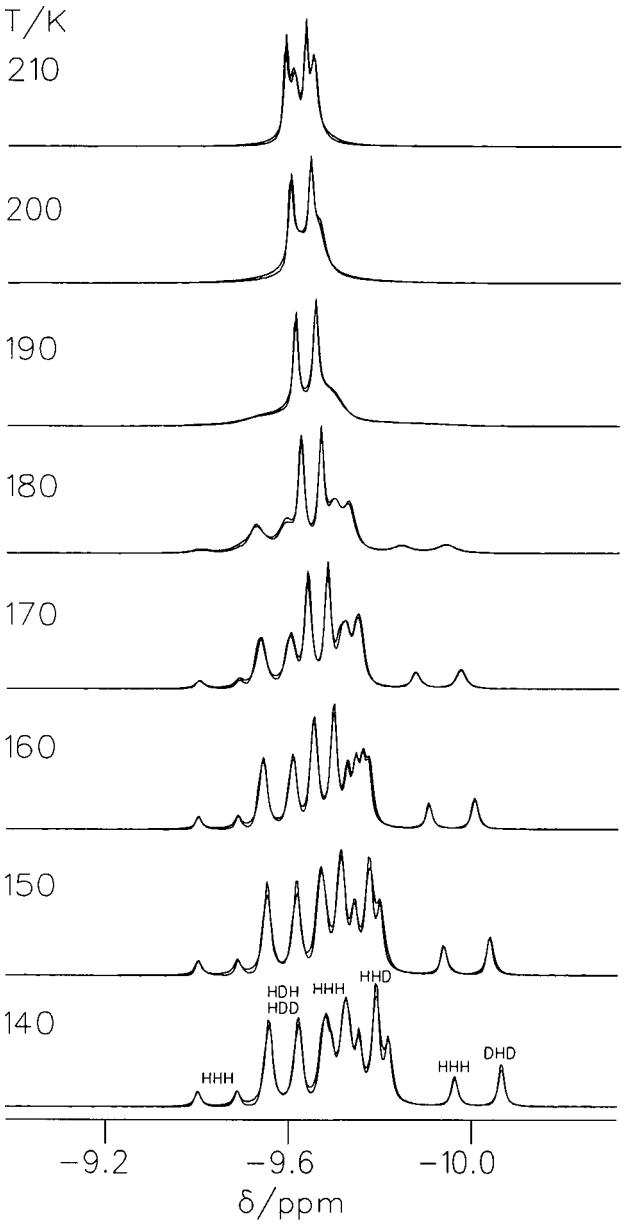

Fig. 4
Superimposed temperature dependent experimental and calculated 500 MHz ^{1}H NMR hydride signals of 35% deuterated $Cp^*RuH_3(Ppy_3)$ (**1**-d) dissolved in $CDClF_2$-CDF_3 (2:1)

$$\pi J_{12} = 10^{5.7} \exp\left(-5.1\,\mathrm{kJ\,mol^{-1}}/RT\right)\mathrm{Hz},\quad 140\,\mathrm{K} \le T \le 180\,\mathrm{K}\ \text{for}\ \mathbf{1}-\mathrm{d} \tag{2}$$

and

$$k_{12}^{HH} = k_{12}^{HD} = 10^{11.2} \exp\left(-34.3\,\mathrm{kJ\,mol^{-1}}/RT\right)\mathrm{Hz},\quad 180\,\mathrm{K} \le T \le 210\,\mathrm{K}\ \text{for}\ \mathbf{1}, \mathbf{1}-d,\ \text{and}\ \mathbf{1}-\mathrm{d}_2,\ k_{12}^{HH} \approx 20\,\mathrm{s^{-1}}\ \text{at}\ 180\,\mathrm{K} \tag{3}$$

We note that the activation parameters of Eqs. (1) to (3) might be subject to changes the parameters could be obtained in a larger temperature range.

4. Discussion

In this paper, the synthesis, structural characterization and the hydrogen dynamics of a novel trihydride (**1**) containing the Ru-Cp* moiety and the tris(pyrollyl)phosphine ligand have been described. In this section we discuss the molecular properties of **1** in comparison with the analogs **2** and **3** containing the ligands $P(Cy)_3$ and $P(Ph)_3$ (Fig. 1).

The x-ray crystal structure of **1** (Fig. 2) shows that the complex adopts a classical piano-stool configuration, almost identical to the structure of **3** [20a]. The Ru-C distances (2.23–2.29 Å) and the Ru-H distances (1.57(4), 1.60(4) and 1.55(2) Å) are identical to those of $Cp^*RuH_3(PPh_3)$ as are the H-Ru-H angles. Only the Ru-P distance is slightly shorter (2.1798(8) Å compared to 2.252(1) Å). This result demonstrates the absence of significant structural change induced by the better π-accepting properties of the phosphine ligands. A comparison with the structure of **2** was not possible as the latter has not yet been described.

The parameters of the coherent and incoherent dihydrogen exchange, i.e. the exchange couplings J_{12} and rate constants k_{12}^{HH} and k_{12}^{HD} of **1** were determined at low temperatures. The corresponding Arrhenius diagrams are depicted in Fig. 5. Within the margin or error, no kinetic isotope effects could be observed. A similar result was obtained recently also for **2** of which data are included in Fig. 5. To our knowledge, **1** exhibits so far the largest exchange couplings determined up to date for these kind of complexes by ^{1}H NMR, i.e. $J_{12} = 3000$ Hz at 180 K. For comparison, the corresponding values for **3** and **2** are 290 Hz [21] and <20 Hz, respectively. This result is in agreement with the better π-accepting properties of the tris pyrollyl phosphine ligand which reduces the electronic density on the metal.

We note that the proton chemical shifts change after deuteration indicating a different geometry of the partially deuterated complex. The effects are very large for substitution in the central hydrogen site (Table 3). As shown in Fig. 5, the effects of introducing one deuteron into sites 1 or 3 increases J_{12} substantially, here to about 20 to 40%. A similar effect was observed previously for **2** [21] and **3** [6c]. As rate constants of the incoherent exchange have not yet been reported for **3**, we have included in Fig. 5 only the results for **1** and **2**. Firstly, no kinetic HH/HD isotope effect could be observed within the margin of error for both molecules. However, we observe that in the case of **1** not only J_{12} but also the k_{12}^{HH} values are much larger as compared to **2**. This indicates that both quantities are related indirectly to the same energy barrier of the dihydrogen exchange although the energies of activation characterizing J_{12} and k_{12}^{HH} are very different. As the different ligands do not substantially change the molecular structure of the molecular ground state they must have a large influence on the electronic structure of the transition state of the exchange.

In order to interpret the experimental findings we firstly will discuss a simple physical model of both the coherent

Table 3
Parameters of the 500 MHz ^{1}H NMR lineshape analysis of a sample of $Cp^*RuH_3(Ppy_3)$ (**1**) dissolved in $CDClF_2$-CDF_3 (2:1)

T/K	δ_1/ppm **1**-hhh	δ_2/ppm **1**-hhh	J_{12}/Hz **1**-hhh	k_{12}^{HH}/s^{-1} **1**-hhh	J_{1P}/Hz **1**-hhh	J_{2P}/Hz **1**-hhh
140	–9.568	–9.948	950	≈0	31	≈0
150	–9.558	–9.912	1500	≈0	31	≈0
160	–9.548	–9.880	1800	≈0	31	≈0
170	–9.540	–9.848	2500	≈0	31	≈0
180	–9.532	–9.822	3000	15	32	≈0
190	–9.526	–9.794	3800[a])	65	32	≈0
200	–9.520	–9.770	4200[a])	150	31	≈0
210	–9.514	–9.754	5300[a])	430	32	≈0

[a]) Extrapolated from lower temperatures according to Eq. (1). The margins of error of the various parameters were not determined, but are estimated to be of the order of 10% to 20% for J_{12} and k_{12}^{HH} which includes that temperature calibration error. In the temperature range between 180 K and 210 K the natural line widths were determined from the inner signal components which are unaffected by the incoherent exchange.

Table 4
Parameters of the 500 MHz ^{1}H NMR lineshape analysis of a sample of partially deuterated $Cp^*RuH_3(Ppy_3)$ (**1**-d) dissolved in $CDClF_2$-CDF_3 (2:1)

T/K	δ_1-Hz **1**-hhh	δ_2/Hz **1**-hhh	$\Delta\delta_1$/ ppm **1**-hhd	$\Delta\delta_2$/ ppm **1**-hhd	$\Delta\delta_1$/ ppm **1**-hdh	$\Delta\delta_1$/ ppm **1**-ddh	$\Delta\delta_2$/ ppm **1**-dhd	J_{12}/Hz **1**-hhh	J_{12}/Hz **1**-hhd	k_{12}^{HH}/s^{-1} **1**-hhh **1**-hhd	k_{12}^{HD}/s^{-1} 1 **1**-hhd	J_{1P}/Hz **1**/hhh	J_{1P}/Hz **1**/hhh	J_{1P}/Hz **1**-hdh	J_{1P}/Hz **1**-hhh
140	–9.566	–9.940	≈0[b])	–0.038	–0.012	–0.018	–0.084	1100	1400	≈0	≈0	31	31	31	31
150	–9.560	–9.916	≈0[b])	–0.038	–0.014	–0.018	–0.096	1500	1600	≈0	≈0	31	29	31	31
160	–9.552	–9.884	≈0[b])	–0.036	–0.012	–0.018	–0.096	2000	2300	2	2	31	29	31	31
170	–9.546	–9.856	≈0[b])	–0.038	–0.012	–0.018	–0.094	2800	3200	8	8	31	29	31	31
180	–9.538	–9.826	≈0[b])	–0.036	–0.008	–0.012	–0.094	3400	4000	30	26	31	30	31	31
190	–9.532	–9.800	≈0[b])	–0.040	–0.010	–0.016	–0.096	4200[a])	4900[a])	110	110	31	30	31	31
200	–9.528	–9.776	≈0[b])	–0.036	–0.008	–0.014	–0.092	5000[a])	5800[a])	300	300	31	30	31	31
210	–9.526	–9.746	≈0[b])	–0.038	–0.010	–0.012	–0.100	6000[a])	6800[a])	790	790	31	30	31	31

$\Delta\delta_i = \delta_i(D) - \delta_i(H)$.
[a]) Extrapolated from lower temperatures according to Eq. (1).
[b]) In contrast to the AB_2X spin system of **1**-hhh, the chemical shifts δ_1 and δ_2 could not be determined by lineshape analysis without assumptions in the case of the ABX-type spin system of **1**-hhd because of the large value of J_{12}. Therefore, we assumed that $\mathbf{d}_1$ is not affected by partial deuteration in the distant site 3. With this assumption all other parameters could be obtained by simulation without assumptions. The margins of error of the various parameters were not determined, but are estimated to be of the order of 10 to 20% for J_{12} and k_{12}^{HH} which includes the temperature calibration error.

and the incoherent processes described in previous work [22, 6c]. In Fig. 6 are depicted the potential energies, energies and wave functions of various rotational states for a non-rigid dihydrogen rotor. The barrier of rotation decreases (Fig. 6a to c) when the distance between the hydrogen atoms is decreased by increasing their distance to the metal. The energy levels come out as pairs split by the frequency J_n. The states which are symmetric with respect to a 180° rotation are linked via the Pauli exclusion principle to the antisymmetric spin states, also called the p-H_2 state, whereas the antisymmetric states are linked to the symmetric splin states o-H_2. The exchange couplings in NMR correspond to tunnel splittings averaged by fast vibrational relaxation over many rovibrational states. It has been argued [22] that "vertical" excitation, e.g. within the configuration of Fig. 6a leads to a decrease of J with increasing temperature, as depicted schematically in Fig. 6d, whereas "horizontal" excitation in the rovibrational groundstate to dihydrogen configurations as indicated in Fig. 6b and 6c should lead to an increase with temperature as depicted in Figs. 6e and 6f. Only an increase is compatible with the experimental findings. When comparing for example **1** and **2**, it follows that the rotational barriers are smaller in the first case as the J are larger.

In the szenario of Fig. 6 the incoherent exchange is not yet included. A detailed description of both processes was proposed recently by Szymanski [6a] and Meyer et al. [6b]. Inspired by this work, we have recently proposed a simplified model (6c) illustrated in Fig. 7. We consider two hydrides bound to a transition metal in two inequivalent sites. We assume that it is possible to label the hydrides as H_a and H_b – for example in a magnetic field by different spins – leading to two quasi-degenerate well-distinguishable ground states A and A′ which differ only in the hydrogen arrangement. The energy difference is small, i.e. of the order of kHz corresponding to typical chemical shift differences in NMR, but larger than the exchange

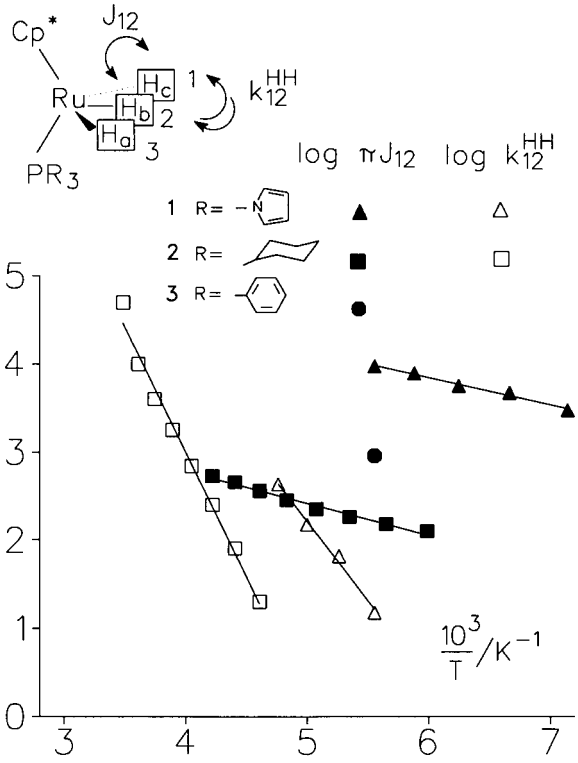

Fig. 5
Arrhenius diagram of the coherent and incoherent dihydrogen exchange in **1** (this study) and **2** (adapted from Ref. [7c])

coupling J_A, assumed to be very small. Via an incoherent process characterized by rate constants k_{AB} and k_{BA} we let the system reach an excited state B which is now strongly coupled to B′, where the energy splitting corresponds to the frequency of the coherent exchange i.e. the exchange coupling J_B. After excitation, B and B′ will interconvert periodically with J_B until desactivation occurs to A or A′. This will lead to a decay of the oscillation between B and B′.

A simple kinetic treatment where the steady state approximation has been applied to the excited state – which implies that this state is present only in a very small concentration – leads to the following expressions for the interconversion between A and A′ via the excited states B and B′ [6c], i.e.

$$\pi J = \frac{\pi J_B \, k_{AB} \, k_{BA}}{k_{BA}^2 + 4\pi^2 J_B^2} \tag{4}$$

and

$$k = \frac{2\pi^2 J_B^2 \, k_{AB}}{k_{BA}^2 + 4\pi^2 J_B^2} \, , \tag{5}$$

where

$$k_{AB} = k_{BA} \, p_B / p_A \approx k_{BA} \, p_B \, , \quad p_B = \exp\left(-E_B / RT\right) \tag{6}$$

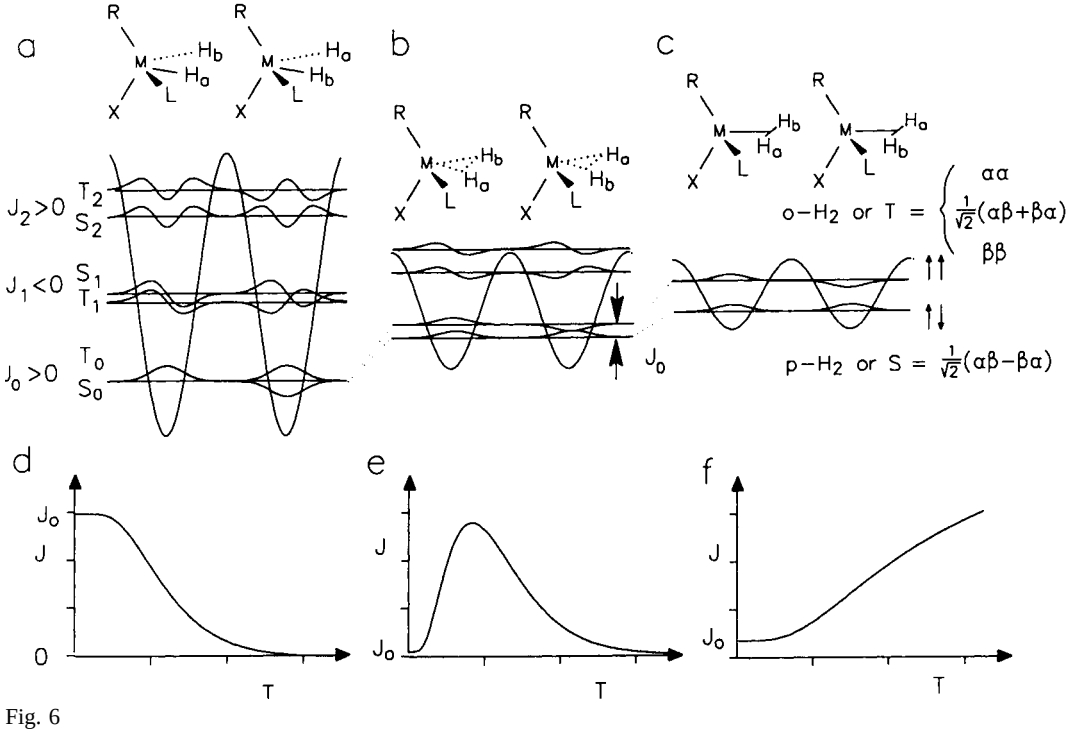

Fig. 6
Potential energies and nuclear wave functions (schematically) of a hindered dihydrogen quantum rotor in a transition metal hydride according to Ref. [5] as a function of the H…H distance. The states occur in pairs consisting of a nuclear singlet and a nuclear triplet state S_n and T_n, with the energy difference or tunnel splitting J_n. The spatial parts of S_n and of T_n are symmetric or antisymmetric with respect to a 180° rotation. For a dihydride configuration (a) the barrier is large but decrease in stretched (b) and a non-stretched dihydrogen configurations (c). In the same sequence the ground state rotational splitting J_0 increases. Note that the number of state pairs n is arbitrary and may be larger than indicated. (d) to (f) Average exchange couplings as a function of temperature

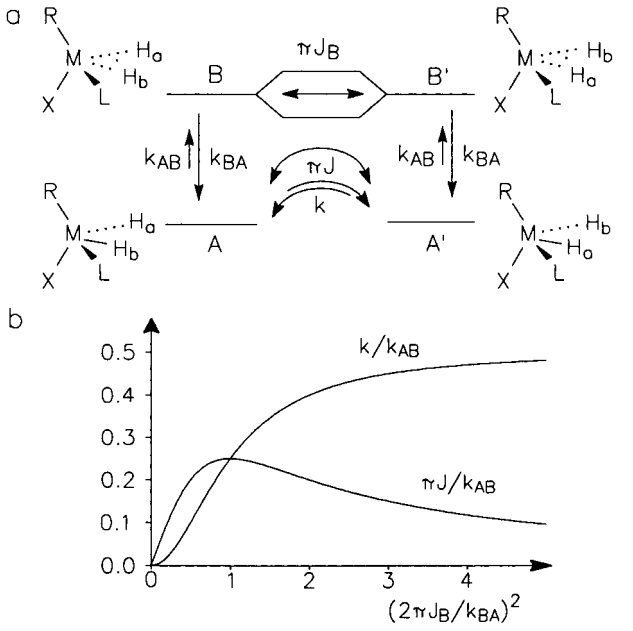

Fig. 7
Average exchange coupling constant πJ and rate constant k in units according to Eqs. (4) and (5) of the exchange between A and A′ via an incoherent activation to B and a coherent or periodic exchange between B and B′ according to Fig. 2a, as a function of $2\pi J_B/k_{BA}$. For further explanation see text

k represents the average rate constant for the incoherent interconversion between A and A′ via the excited states B and B′ and J the average frequency of the coherent or periodic interconversion. p_B is the Boltzman factor of the excited states exhibiting the average energy E_B. Both J and k are measured by NMR and INS [6c] and included in Fig. 5. Whereas J_B is temperature independent, and k_{BA} only slightly temperature dependent, k_{AB} is strongly dependent on temperature because of the Boltzmann factor. Thus, the temperature dependence of both k and J is given to a good approximation by E_B. Moreover, a plot of log k and log πJ vs. $1/T$ should show an Arrhenius-type behavior. In Fig. 7b we plot k and J as a function of the ratio $2\pi J_B/k_{BA}$. In the coherent exchange regime where $(2\pi J_B/k_{BA})^2 \ll 1$, it follows that

$$k = (2\pi J_B)^2 p_B/k_{BA} \ll \pi J = p_B J_B\,, \qquad (7)$$

Now, A and A′ interconvert periodically via the states B and B′. In the incoherent exchange regime where $(2\pi J_B/k_{BA})^2 \gg 1$ we obtain

$$k = k_{AB}/2 = p_B\, k_{BA}/2 \gg \pi J = k_{AB}\, k_{BA}^2/4\pi J_B\,. \qquad (8)$$

Now, during the lifetime of the excited state B and B′ interconvert periodically very often until the system reacts either to A or to A′ with equal probabilities, and the contribution of the excited state to J becomes very small.

Finally, we note that in practice a large number of excited states B with different energies E_B has to be considered which leads in principle to a non-Arrhenius behavior of both J and k. However, in practice data have to be accumulated in a very large temperature range in order to detect such a non-Arrhenius behavior. Therefore, the model of Fig. 7 should be a good approximation when a relatively small temperature range is considered.

A look at the Arrhenius diagram shows, however, that the energy of activation which determines the temperature dependence of k is much larger than the energy determining the temperature dependence of J. Within the simple model of Fig. 7, the pre-exponential factor of about $10^{11.2}$ s^{-1} for the incoherent process (Eq. (3)) may be identified with half of k_{AB}, the rate of desactivation to the ground state. This means that $10^{11.5} \ll \pi J_B$, which must then be of the order of 10^{13} s^{-1}, i.e. of the order of a vibrational frequency. As a consequence, the state which determines the temperature dependence of k must be located close to the top of the barrier of the dihydrogen rotation, and may, therefore, be also called the "transition state" of the incoherent exchange. The transition state cannot contribute to J any longer. Therefore, the levels responsible for the temperature dependence of πJ must be located well below the top of the barrier as they must exhibit tunnel splittings which are much smaller than 10^{11} s^{-1}. This condition is fulfilled for the typical values of 10^6 Hz as indicated by the pre-exponential factors of Eqs. (1) and (2). Thus, it becomes clear that at low temperature $k \ll \pi J$ but that at higher temperatures $k \gg \pi J$.

The observation that there is no kinetic HH/HD isotope effect on the incoherent exchange is, at first sight unexpected. A large effect should have been observed if the states which govern the temperature dependence of k are located below the barrier, as the interconversion between B and B′ should be much slower in the case of a HD-pair as compared to the HH-pair because of the larger tunneling mass. Moreover, the HD exchange between B and B′ will not be coherent but an incoherent rate process. For the reaction over the barrier one would normally also expect an HH/HD isotope effect on the incoherent exchange, arising from differences in zero-point energies between the excited "transition" state and the ground state, for a dihydrogen configuration as transition state. If this mechanism is true, the finding that no isotope effect can be observed within the margin of the experimental error indicates some compensation of zero-point energies between the groundstate and the transition state. This could happen as the HH-bond is strengthened as the M-H bonds are weakened.

Conclusions

We describe in this article the synthesis of a new trihydride complex containing the pentamethylcyclopentadienyl ligand (Cp*) and its deuterated analogs. The originality of this compounds is to contain a new electron withdrawing phosphine ligand, tris(pyrollyl)phosphine (Ppy_3) which displays steric properties very similar to triphenylphosphine. This allows a direct comparison of the spectroscopic properties and of the reactivity of both series of

compounds. No significant structural differences were found between $Cp^*RuH_3(Ppy_3)$ (**1**) and $Cp^*RuH_3(PPh_3)$ (**3**) and, in particular, both compounds are formally ruthenium IV trihydrides. However, we found that **1** displays exchange couplings and rate constants of the incoherent exchange which are significantly larger than for $Cp^*RuH_3(PCy_3)$ (**2**) and for **3**. This indicates the presence of a lower barrier for the classical exchange of hydrogen in the case of **1** which is consistent with the presence of a reduced electron density on **1** compared to **3**. The kinetic results are rationalized in terms of a simple model where an incoherent excitation to an excited state exhibiting a large exchange coupling may either contribute to the average exchange coupling or to the average rate constants of the incoherent exchange, depending on the lifetime of the state as compared to its exchange coupling. In principle, this mechanism should lead to an observable kinetic HH/HD isotope effect on the incoherent exchange at low temperatures. Apparently, even in the case of **1** which exhibits the largest known exchange couplings observed by NMR this regime could not yet been reached.

We are very grateful to Dr. Gerd Buntkowsky, Free University of Berlin, Prof. R.R. Ernst and Prof. R. Meyer, R. Wiedenbruch and Ch. Scheurer, all ETH Zürich, for stimulating discussions. This work was supported by the European Community Human Capital & Mobility Network "Localization and Transfer of Hydrogen" (No. CHRX CT 940582) and the Deutsche Forschungsgemeinschaft, Bonn/Bad Godesberg. H.H.L. also thanks the Fonds der Chemischen Industrie, Frankfurt, for financial support.

References

[1] a) R.H. Crabtree, Angew. Chem. Int. Ed. Engl. *32*, 789 (1993); b) X.-L. Luo, G.J. Kubas, J.C. Bryan, C.J. Burns, and C.J. Unkefer, J. Am. Chem. Soc. *116*, 10312 (1994); c) G.J. Kubas, Acc. Chem. Res. *21*, 120 (1988); d) R.H. Crabtree, Acc. Chem. Res. *23*, 95 (1990); e) P.G. Jessop and R.H. Morris, Coord. Chem. Rev. *121*, 155 (1992); f) D.M. Heinekey and W.C. Oldham Jr., Chem. Rev. *93*, 913 (1993).

[2] J. Eckert and G.J. Kubas, J. Phys. Chem. *97*, 2378 (1993).

[3] a) F.A. Jalon, B. Manzano, A. Otero, E. Villasenor, and B. Chaudret, J. Am. Chem. Soc. *117*, 10123 (1995); b) S. Sabo-Etienne, B. Chaudret, H. Abou el Makarim, J.-C. Barthelat, J.-P. Daudey, S. Ulrich, H.-H. Limbach, and C.J. Moise, J. Am. Chem. Soc. *117*, 11602 (1995).

[4] Some leading references on exchange couplings (complexes, NMR origin and quantum mechanical calculations). a) T. Arliguie, B. Chaudret, J. Devillers, and R. Poilblanc, R.C.R. Hebd.Séances Acad. Sci. *305-II*, 1523 (1987); b) T. Arliguie, B. Chaudret, F. Jalón, A. Otero, J.A. López, and F.J. Lahoz, Organometallics *10*, 1888 (1991); c) B. Chaudret, H.-H. Limbach, and C. Moise, C.R. Séances Acad. Sci. *513-II*, 533 (1992); d) A. Antiñolo, F. Carrillo, B. Chaudret, J. Fernández-Baeza, M. Lafranchi, H.-H. Limbach, M. Maurer, A. Otero, and M.A. Pellinghelli, Inorg. Chem. *35*, 7873 (1996); e) K.W. Zilm, D.M. Heinekey, J.M. Millar, N.G. Payne, and P. Demou, J. Am. Chem. Soc. *111*, 3088 (1989); f) K.W. Zilm, D.M. Heinekey, J.M. Millar, N.G. Payne, S.P. Neshyba, J.C. Duchamp, and J. Szcyrba, J. Am. Chem. Soc. *112*, 920 (1990); g) D.M. Heinekey, J. Am. Chem. Soc. *113*, 6074 (1991), h) D.H. Jones, J.A. Labinger, and D.P. Weitekamp, J. Am. Chem. Soc. *111*, 3087 (1989); i) D.G. Gusev, R. Kuhlman, G Sini, O. Eisenstein, and K.G. Caulton, J. Am. Chem. Soc. *116*, 2685 (1994); j) B. Manzano, F. Jalon, S. Sabo-Etienne, B. Chaudret, S. Ulrich, and H.-H. Limbach, J. Chem. Soc. Dalton Trans. *1997*, 3153.

[5] a) H.-H. Limbach, G. Scherer, L. Meschede, F. Aguilar-Parrilla, B. Wehrle, J. Braun, C. Hoelger, H. Benedict, G. Buntkowsky, W.P. Fehlhammer, J. Elguero, J.A.S. Smith, and B. Chaudret, NMR Studies of Elementary Steps of Hydrogen Transfer in Condensed Phases, in: Y. Gauduel and P.J. Rossky (eds.) Ultrafast Reaction Dynamics and Solvent Effects, American Institute of Physics, AIP Conference Proceedings, Part III, *298*, 225–239 (1994); b) A. Antiñolo, F. Carrillo, B. Chaudret, M. Fajardo, J. Fernandez-Baeza, M. Lanfranchi, H.-H. Limbach, M. Maurer, A. Otero, and M.A. Pellinghelli, Inorg. Chem. *33*, 5163 (1994).

[6] a) S. Szymanski, J. Chem. Phys. *104*, 8216 (1996); b) C. Scheurer, R. Wiedenbruch, R. Meyer, and R.R. Ernst, J. Chem. Phys. *106*, 1 (1996); c) H.-H. Limbach, S. Ulrich, G. Buntkowsky, S. Sabo-Etienne, B. Chaudret, G.J. Kubas, and J. Eckert, J. Am. Chem. Soc., submitted for publication; d) G. Buntkowsky, H.H. Limbach, F. Wehrmann, I. Sack, H.M. Vieth, and R.H. Morris, J. Phys. Chem. A. *101*, 4679 (1997).

[7] J.A. Ayllon, S. Sabo-Etienne, B. Chaudret, S. Ulrich, and H.-H. Limbach, Inorg. Chim. Acta *259*, 1 (1997).

[8] M. Kranenburg, P.C.J. Kamer, P.W.N.M. Van Leeuwen, and B. Chaudret, J. Chem. Soc. Chem. Comm. *1997*, 373.

[9] See for example: a) B. Chin, A.J. Lough, R.H. Morris, C.T. Schweitzer, and C. D'Agostino, Inorg. Chem. *33*, 6278 (1994); b) E.P. Cappelani, S.D. Drouin, G. Jia, P.A. Maltby, R.H. Morris, and C.T. Schweitzer, J. Am. Chem. Soc. *116*, 3375 (1994).

[10] K.G. Moloy and J.L. Petersen, J. Am. Chem. Soc. *117*, 7696 (1995).

[11] S. Serron, S.P. Nolan, and K.G. Moloy, Organometallics *15*, 4301 (1996).

[12] a) T.D. Tilley, R.H. Grubbs, and J.E. Bercaw, Organometallics *3*, 264 (1984); b) N. Oshima, H. Suzuki, and Y. Moro-Oka, Chem. Lett. *1984*, 1161.

[13] a) G.S. Denisov and N.S. Golubev, J. Mol. Struct. *75*, 311 (1981); b) N.S. Golubev, S.F. Bureiko, and G.S. Denisov, Adv. Mol. Relax. Inter. Proc. *24*, 225 (1982); c) N.S. Golubev; G.S. Denisov, and E.G. Pushkareva, J. Mol. Liquids *26*, 169 (1983); d) N.S. Golubev and G.S. Denisov, J. Mol. Struct. *270*, 263 (1992); e) N.S. Golubev, S.N. Smirnov, V.A. Gindin, G.S. Denisov, H. Benedict, and H.-H. Limbach, J. Am. Chem. Soc. *116*, 12055 (1994).

[14] a) G. Binsch, J. Am. Chem. Soc. *91*, 1304 (1969); b) J.W. Emsely, J.L. Feeney, and H. Sutcliffe, High Resolution Nuclear Magnetic Resonance Spectroscopy, Vol. 1, Pergamon Press, Oxford 1965; c) A. Abragam, The Principles of Nuclear Magnetism, Clarendon Press, Oxford 1961; d) R.R. Ernst, G. Bodenhausen, and A. Wokaun, Principles of NMR in One and Two Dimensions, Clarendon Press, Oxford 1987.

[15] A. Altomare, G. Cascarano, G. Giacovazzo, A. Guagliardi, M.C. Burla, G. Polidori, and M. Camalli, J. Appl. Crystallogr. *27*, 435 (1994).

[16] E. Prince, Mathematical Techniques in Crystallography, Springer-Verlag, Berlin, 1982.

[17] D.J. Watkin, C.K. Prout, R.J. Carruthers, and P. Betteridge, CRYSTALS Issue 10, Chemical Crystallography Laboratory, Oxford, UK, 1996.

[18] D.J. Watkin, C.K. Prout, and L.J. Pearce, CAMERON, Chemical Crystallography Laboratory, Oxford, UK, 1996.

[19] International Tables for X-Ray Crystallography, Vol. IV, Kynoch Press, Birmingham, England, 1974.

[20] a) H. Suzuki, D.H. Lee, N. Oshima, and Y. Moro-Oka, Organometallics, *6*, 1569 (1987); b) T. Arliguie, C. Border, B. Chaudret, J. Devillers, and R. Poilblanc, Organometallics *8*, 1308 (1989).

[21] D.M. Heinekey, N.G. Payne, and C.D. Sofield, Organometallics *9*, 2643 (1990).

[22] a) H.-H. Limbach, G. Scherer, M. Maurer, and B. Chaudret, Angew. Chem. Int. Ed. Engl. *31*, 1369 (1992); b) J.C. Barthelat, B. Chaudret, J.P. Daudey, P. De Loth, and R. Poilblanc, J. Am. Chem. Soc. *113*, 9896 (1991); c) E. Clot, C. Leforestier, O. Eisenstein, and M. Pélissier, J. Am. Chem. Soc. *117*, 1797 (1995); d) A. Jarid, M. Moreno, A. Lledos, J.M. Lluch, and J. Bertran, J. Am. Chem. Soc. *117*, 1069 (1995).

Presented at the Discussion Meeting of the Deutsche Bunsen-Gesellschaft für Physikalische Chemie “Hydrogen Transfer: Experiment and Theory” in Berlin, September 10th to 13th, 1997

E 9755